J Inorg Organomet Polym (2012) 22:119–124
DOI 10.1007/s10904-011-9507-5

Preparation of Transparent PVC-Titanosilicate Nanocomposites by Interlamellar Silylation of Layered Titanosilicate

Kyeong-Won Park · Jong Hwa Jung

Received: 28 March 2011 / Accepted: 10 June 2011 / Published online: 14 July 2011

Abstract The preparation and structural characterization of a transparent poly(vinyl chloride)–octyltriethoxysilane-Jilin Davy Faraday-Layered solid #1 nanocomposite is reported. H^+-Jilin Davy Faraday-Layered solid #1 ($H_4Ti_2Si_8O_{22}$) was prepared by proton exchange of layered Na^+-Jilin Davy Faraday-Layered solid #1 ($Na_4Ti_2Si_8O_{22}$). The octyltriethoxysilane-Jilin Davy Faraday-Layered solid #1, in a siloxane-pillared form, was obtained by hydrolysis of the H^+-Jilin Davy Faraday-Layered solid #1–dodecylamine–octyltriethoxysilane in pure water. In addition, the poly(vinyl chloride)–octyltriethoxysilane-Jilin Davy Faraday-Layered #1, as an organic–inorganic nanocomposite, was prepared using a poly(vinyl chloride) resin and Na^+-Jilin Davy Faraday-Layered solid #1, H^+-Jilin Davy Faraday-Layered solid #1 or octyltriethoxysilane-Jilin Davy Faraday-Layered #1 in tetrahydrofuran. The prepared organic–inorganic nanocomposite, as an interlayer space expander, was confirmed by XRD, SEM, EDS, TGA and TEM. The poly(vinyl chloride)–octyltriethoxysilane-Jilin Davy Faraday-Layered #1 nanocomposite showed a larger interlayer distance (~6.74 nm) than octyltriethoxysilane-Jilin Davy Faraday-Layered solid #1 (2.95 nm), H^+-Jilin Davy Faraday-Layered solid #1 (0.92 nm) and Na^+-Jilin Davy Faraday-Layered solid #1 (1.08 nm).

Keywords Jilin Davy Faraday-Layered solid #1 · Nanocomposites · Intercalation · Transparent · Poly(vinyl chloride)-Jilin Davy Faraday-Layered solid #1 nanocomposites · XRD

K.-W. Park (✉) · J. H. Jung
Department of Chemistry, Research Institute of Natural Science, Gyeongsang National University, Jinju 660-701, Republic of Korea
e-mail: nano2k@nate.com

1 Introduction

Polymer-layered silicate nanocomposites have attracted great interest from academic and industrial researchers over the past decade [1–3]. Many polymer-layered silicate nanocomposites have been reported, including polypropylene [4], polystyrene [5, 6], poly(methylmethacrylate) [7, 8], polyimide [9] and epoxy resin [10]. Poly(vinyl chloride) (PVC), as an important commercial polymer, has been studied and used widely for many years. However, due to its inherent disadvantages, such as low thermal stability and brittleness, PVC and its composites are subject to some application limitations [11]. Therefore, it is worthwhile to develop new PVC products with properties that will add high value and broaden applications.

Recently, the development of polymer-layered silicate nanocomposites presents a new way to prepare high performance PVC composites. PVC/nano-$CaCO_3$ and PVC/cellulose whisker nanocomposites have been reported [12, 13]. In contrast, PVC/montmorillonite nanocomposites have not drawn much attention, except for a few publications on PVC-layered silicate nanocomposites [14]. Layered silicate has been often used to design and construct organic–inorganic nanomaterials because of the ease and variety of modifications possible by the introduction of organic and inorganic compounds into the interlayer space [15–17]. Microporous titanosilicate contributes significantly to the field of materials science-inorganic polymers, especially for liquid phase partial oxidation reactions [18, 19]. Recently, we have reported the silylation of octyltriethoxysilane (OTES) on the interlayer surface of H^+-Jilin Davy Faraday-Layered solid #1 (H^+-JDF-L1) [20]. Na^+-Jilin Davy Faraday-Layered solid #1 (Na^+-JDF-L1) is a layered titanosilicate that can be synthesized under hydrothermal conditions. In particular, a general synthetic

strategy was developed during the studies of JDF-L1 ($Na_4Ti_2Si_8O_{22}{\cdot}4H_2O$) by Robert et al. [21]. Ferdov et al. also reported a convenient preparation of JDF-L1 [22], which contains Na^+-JDF-L1 layers composed of tetrahedral SiO_4 units and square pyramidal TiO_5 polyhedrons [21]. The interlayer surfaces are composed of five-coordinate Ti(V) and, thus, have a smaller coordination number than the octahedrally coordinated microporous and layered Na^+-JDF-L1 [21]. The titanium in JDF-L1 is five-coordinate and has excellent catalytic ability for oxidation reactions [22]. Each layer is separated by water molecules around an interlayer of Na^+ ions [23]. This layering structure allows the intercalation of large organic and inorganic molecules.

OTES has been extensively used for the chemical modification of silica, alumina and titanium surfaces [20]. Moreover, the interlayer surfaces of acid-treated layered silicates in OTES consist of very accessible and reactive Si–OH groups. OTES can also intercalate directly into the interlayer of acid-treated layered silicates to react with Si–OH and Ti–OH groups. Previously, we reported the synthesis and characterization of OTES-JDF-L1 [20]. In this paper, we studied the preparation of transparent PVC–OTES-JDF-L1 nanocomposites by mixing PVC and OTES-JDF-L1 in THF. The mixture was added to a glass circular mold. Then, the solvent in a circular mold was evaporated at room temperature. A transparent PVC nanocomposite was obtained with a thickness of $\sim$1 mm and contained titanosilicate (PVC–OTES-JDF-L1).

2 Experimental Section

2.1 Materials

Reagent grade chemicals and solvents were used as received without further purification. SiO_2 (particle size 200 μm, Merck), NaOH (Junsei, Japan), $TiCl_4$ (Yakuri Pure Chemicals Co., Japan) and octyltriethoxysilane (97.5%), dodecylamine (98%) and HCl 3(7%) were purchased from Aldrich. High relative molecular weight PVC was obtained from Fluka and EtOH (95%) (Daejeong chemical Co., Korea) were used as received.

2.2 Synthesis of Na^+-JDF-L1 and H^+-JDF-L1

Na^+-JDF-L1 was hydrothermally synthesized from SiO_2, NaOH, $TiCl_4$ and water using methods developed in our laboratory [20, 24]. The experiment was carried out in a stainless steel autoclave (50 h, 180 °C, autogenous pressure) without stirring. The product was filtered and washed with deionized water to remove excess NaOH and Cl^- and dried at 70 °C. H^+-JDF-L1 was obtained using ion exchange of Na^+ in Na^+-JDF-L1 by H^+ with a 0.1 N HCl solution. A suspension of Na^+-JDF-L1 (10 g) in deionized water (200 mL) was titrated slowly with a 0.1 N HCl solution to a final pH of 2.0 and then maintained at room temperature with stirring for 24-h. The H^+-JDF-L1 was recovered by filtering, washing with deionized water (until Cl^- free), and air drying at 40 °C.

2.3 Silylation of H^+-JDF-L1

OTES-JDF-L1 derivatives were prepared using methods reported previously [20], which introduced OTES and dodecylamine (DDA) into the interlayer regions of H^+-JDF-L1 without a separate pre-swelling step. DDA–OTES-mixed solutions were prepared by dissolving OTES and DDA in 95% ethanol. The concentration of OTES and DDA in solution was 0.1 M. H^+-JDF-L1, intercalated with OTES and DDA (DDA–OTES-JDF-L1), was prepared by dispersion of H^+-JDF-L1 (0.321 g, 0.5 mmol) in 6 mL, 0.1-M OTES (3 mL) and 0.1 M DDA (3 mL) (ultrasound, 20 min, at room temperature) and evaporated and dried for 24-h at 50 °C. OTES-JDF-L1 was prepared by filtering and washing with ethanol until DDA was removed from DDA–OTES-JDF-L1 and then drying in air at 70 °C.

2.4 Preparation of PVC Nanocomposites

The organic–inorganic PVC nanocomposite was prepared by PVC powder (0.2 g) and inorganic materials (0.066 g); for example, (a) Na^+-JDF-L1, (b) H^+-JDF-L1, (c) OTES-JDF-L1 were mixed and dissolved in THF (5.0 mL). The resulting solution was poured onto a glass ring with an inner diameter of 35 mm resting on a smooth glass plate. THF was allowed to evaporate for 48-h at room temperature. The transparent PVC nanocomposite films had a thickness of $\sim$1 mm.

2.5 Characterization

Powder X-ray diffraction (XRD) patterns were obtained using a Bruker AXS D8 DISCOVER diffractometer with Cu Kα (0.1542 nm) radiation. The data were collected in the WAXS 2θ range: 5–65°, SAXS 2θ range: 1–10° with a step size of 0.01° and a count time of 5 s/step. Scanning electron micrographs (SEM) were obtained with a JEOL JSM-840A scanning electron microscope. Transmission electron micrographs (TEM) were obtained with a JEOL JEM-200 CX transmission electron microscope operating at 200 kV and using a thin-section technique. Powdered samples were embedded into epoxy resin and then sectioned with a glass knife. Microtome-sectioned samples

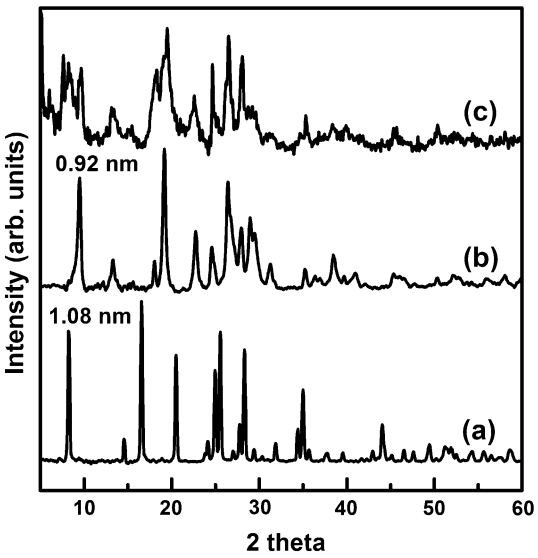

Fig. 1 XRD patterns of (*a*) Na^+-JDF-L1, (*b*) H^+-JDF-L1, and (*c*) OTES-JDF-L1

were examined. The chemical compositions of Na^+-JDF-L1 and H^+-JDF-L1 were analyzed by energy-dispersive X-ray spectrometer (EDS, Link system AS1000-85S). Thermogravimetric analysis (TGA) experiments were carried out at a heating rate of 10 °C/min to 900 °C under a N_2 purge (100 cm^3/min).

3 Results and Discussion

Well crystallized Na^+-JDF-L1 was obtained by the hydrothermal reaction of silica gel for 50-h at 180 °C. The XRD pattern of air-dried Na^+-JDF-L1 exhibited several sharp reflection peaks, indicating a basal spacing of 1.08 nm for [001] (Fig. 1a). On the other hand, due to the loss of interlayer H_2O after exchange, the spacing for air-dried H^+-JDF-L1 decreased slightly to 0.92 nm at 9.6° (Fig. 1b) [24]. For PVC–OTES-JDF-L1, the distance between this layer and the layer of JDF-L1 was 6.74 nm (Fig. 3d), which is ~6 times larger than those of Na^+-JDF-L1 (Fig. 1a) and H^+-JDF-L1 (Figs. 1b, 3a). These findings strongly suggest that the space between one OTES-JDF-L1 layer and another was controlled by intercalation with PVC.

The SEM images of Na^+-JDF-L1 and H^+-JDF-L1 are shown in Fig. 2. Na^+-JDF-L1 particles were composed of plates, with (b) H^+-JDF-L1 and (c) OTES-JDF-L1 exhibiting a similar morphology. In Fig. 2d, composites of PVC–OTES-JDF-L1 are inserted between the layers. As a result the pieces are scattered. The chemical compositions of Na^+-JDF-L1 and H^+-JDF-L1, which were obtained by combining the results of thermogravimetric analysis and EDS analysis (the content of titanium, silica and sodium), are $Na_4Ti_2Si_8O_{22}{\cdot}4H_2O$ and $H_4Ti_2Si_8O_{22}{\cdot}4H_2O$, respectively [21, 24].

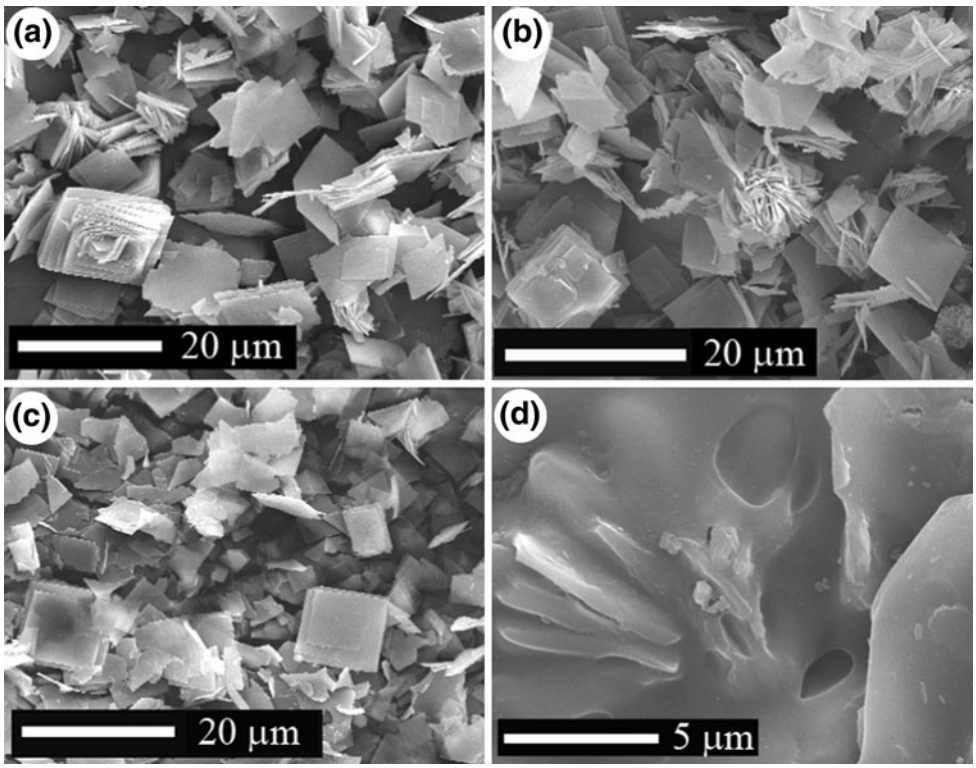

Fig. 2 SEM images of **a** Na^+-JDF-L1, **b** H^+-JDF-L1, **c** OTES-JDF-L1, and **d** PVC–OTES-JDF-L1 nanocomposites

The XRD patterns of DDA–OTES-JDF-L1 treated with a 0.1 M OTES–0.1 M DDA–ethanol solution are shown in Figs. 1c and 3. Treatment of H^+-JDF-L1 with the OTES–DDA mixed solution ensured successful silylation by OTES. Dried OTES–DDA-JDF-L1 powder consists of H^+-JDF-L1 with intercalated OTES and DDA. In the interlayer space, DDA is converted to dodecylammonium cations $CH_3(CH_2)_{11}NH_3^+$ as a result of reaction with acidic silanol groups. Here, condensation between adjacent layers cannot occur because of the large expansion of the interlayer space, with a basal spacing of 3.87 nm (Fig. 3b) by DDA. However, increasing concentrations of OTES broaden the reflections and decrease the basal spacing because of the high degree of grafting that reduces the amount of intercalated DDA. The XRD patterns of DDA–OTES-JDF-L1 after washing with ethanol to remove the DDA showed that increasing the concentration of OTES broadens the reflections and decreases the basal spacing because a high degree of grafting reduces the amount of intercalated OTES (Fig. 3c). The interlayer space had a basal spacing of 2.95 nm (Fig. 3c). This small increase in basal spacing indicates that OTES molecules arrange with a paraffin-type structure. The interlayer space of PVC–OTES-JDF-L1 had a basal spacing of ~6.74 nm (Fig. 3d). The results suggest that the space between layers of OTES-JDF-L1 increases with intercalation of PVC.

TGA data from composites (a) PVC-Na^+-JDF-L1, (b) PVC-H^+-JDF-L1 and (c) PVC–OTES-JDF-L1 under a N_2 purge at a heating rate of 10 °C/min are shown in Fig. 4. The pyrolysis of PVC comprises three weight-loss stages. The weight loss from 100 to 150 °C is ~5.0 wt% and is probably caused by loss of water and solvent that is present between the interlayers. A weight-loss of ~50% from 150 to 350 °C occurs in two stages. The first stage is attributed to the volatilization of hydrogen chloride molecules followed by the formation of the conjugated polyene sequences, while the second stage corresponds to the thermal cracking of the carbonaceous conjugated polyene sequences. The third weight-loss occurs above 500 °C and corresponds to the second pyrolysis of PVC with a weight-loss of ~20%. Figure 5 shows the TEM image obtained from an intercalated and an exfoliated nanocomposite, which, in spite of the partial destruction of the platelets in the outer appearance (see SEM, Fig. 2d), exhibits uniform distance distributions and ordered basal spacing. The cross section of a PVC–OTES-JDF-L1 platelet shows several silicate sheets with a uniform spacing of ~6.74 nm.

Figure 6 are photographs of (a) PVC-Na^+-JDF-L1 (b) PVC-H^+-JDF-L1 and (c) PVC–OTES-JDF-L1, the three main types of composites from Na^+-JDF-L1, H^+-JDF-L1 and OTES-JDF-L1. These composites are obtained

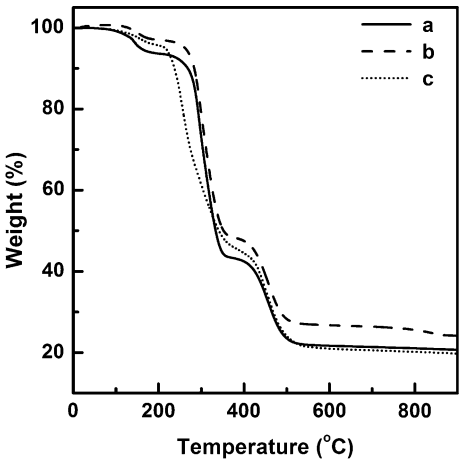

Fig. 4 TGA curves of (*a*) PVC-Na^+-JDF-L1, (*b*) PVC-H^+-JDF-L1, and (*c*) PVC–OTES-JDF-L1 nanocomposites

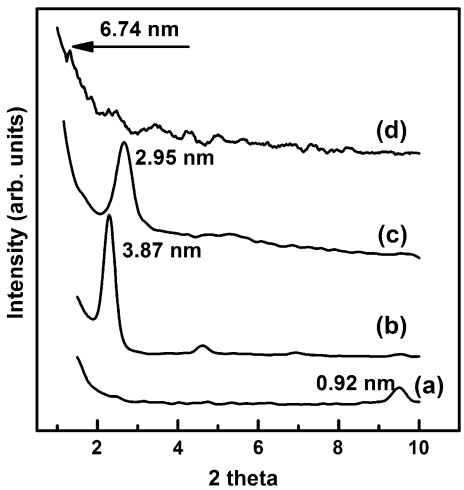

Fig. 3 XRD patterns of (*a*) H^+-JDF-L1, (*b*) DDA–OTES-JDF-L1, (*c*) OTES-JDF-L1, and (*d*) PVC–OTES-JDF-L1 nanocomposites

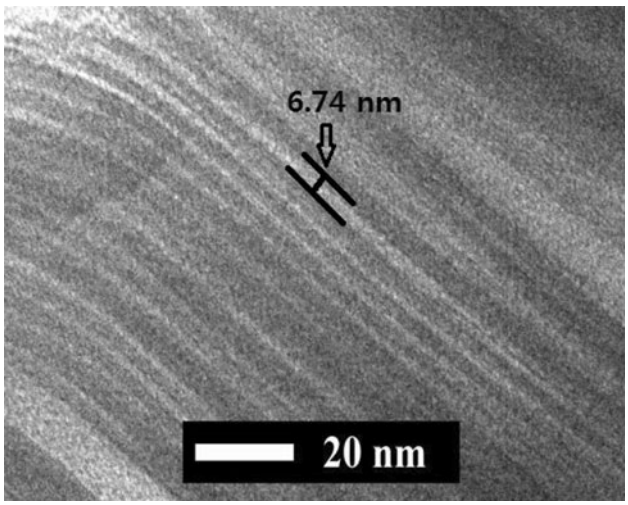

Fig. 5 TEM image of PVC–OTES-JDF-L1 nanocomposites

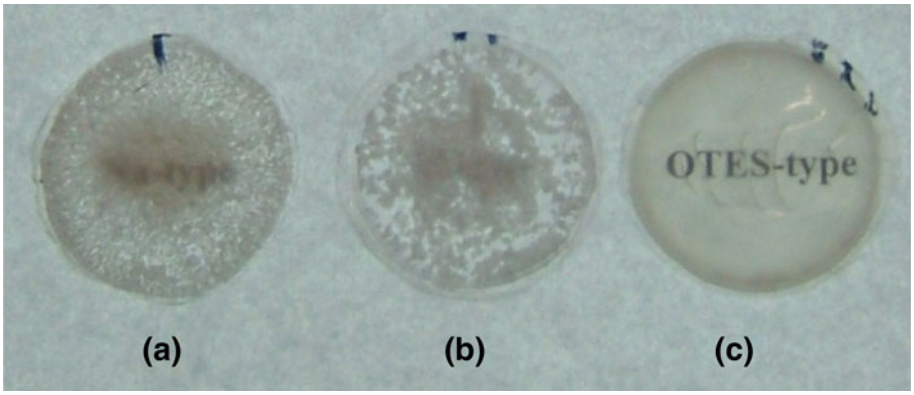

Fig. 6 Photographs of **a** PVC-Na^+-JDF-L1, **b** PVC-H^+-JDF-L1, and **c** PVC–OTES-JDF-L1 nanocomposites, showing the PVC–OTES-JDF-L1 are most transparent among the samples investigated

when layered clay is associated with a polymer. When the PVC is unable to intercalate between the silicates sheets, a phase-separated composite (Fig. 6a, b) is obtained, whose properties are comparable to traditional nanocomposites. Figure 6a and b show that the PVC-Na^+-JDF-L1 and PVC-H^+-JDF-L1 composites are not dispersed and are not transparent. However, in the exfoliated structure (Fig. 6c), a single (and sometimes more than one) extended PVC-polymer chain is intercalated between the OTES-JDF-L1 layers resulting in a well ordered multilayer morphology that is composed of alternating polymer and OTES-JDF-L1. When the OTES-JDF-L1 layers are completely and uniformly dispersed in a continuous polymer matrix, an exfoliated or delaminated structure is obtained (Fig. 6c). Therefore, the PVC–OTES-JDF-L1 membrane is highly transparent, and writing is easily read when viewed through the film.

Figure 7 shows a proposed schematic model for the formation of the polymer-intercalated process. In the PVC solution system, the PVC is not intercalated into the Na^+-JDF-L1 (Fig. 7a) and H^+-JDF-L1 (Fig. 7b) because the hydrophilic Na^+-JDF-L1 and H^+-JDF-L1 are not distributed in the PVC solution. The PVC is intercalated into OTES-JDF-L1 (Fig. 7c), however, because a hydrophobic

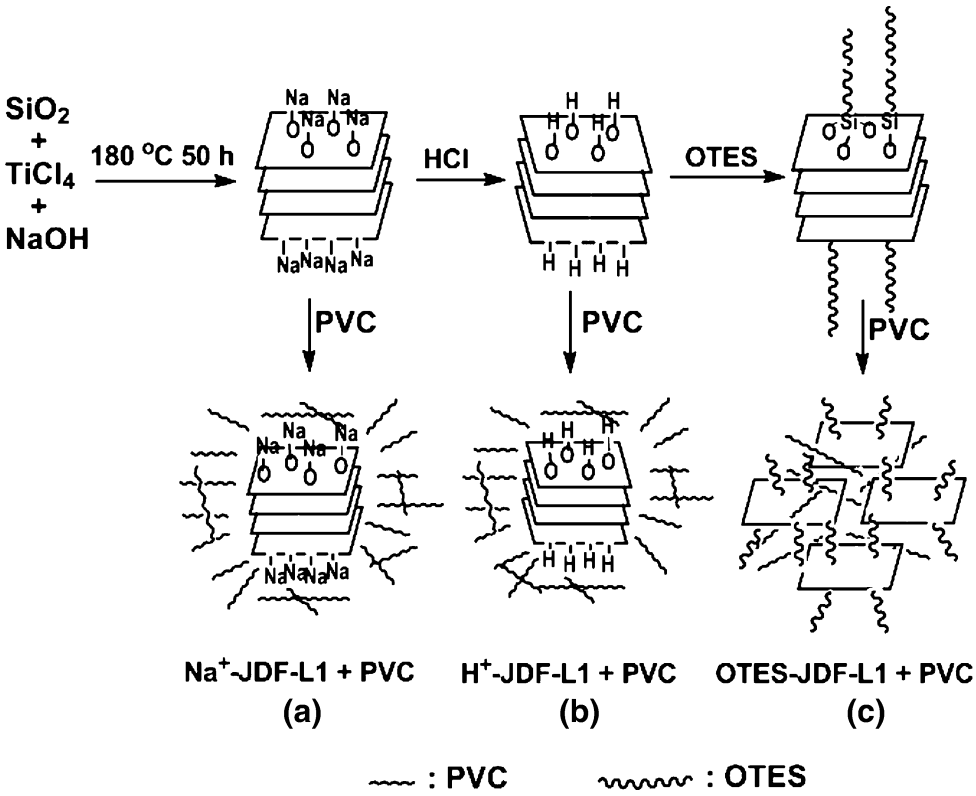

Fig. 7 Schematic representation of PVC–OTES-JDF-L1 nanocomposites

alkyl groups in OTES is attached to the JDF-L1 surface and the OTES-JDF-L1 plates are exfoliated. Therefore, the PVC–OTES-JDF-L1 nanocomposites become transparent.

4 Conclusion

Transparent PVC–OTES-JDF-L1 nanocomposites were easily and simply prepared by intercalation of OTES-JDF-L1 with PVC. The PVC–OTES-JDF-L1 nanocomposites showed much larger interlayer distances ($\sim$6.74 nm at PVC–OTES-JDF-L1 and 2.95 nm at OTES-JDF-L1) than those of H^+-JDF-L1 (0.92 nm) and Na^+-JDF-L1 (1.08 nm). This material, based on the intercalation process, may be a promising route for the development of custom-made nanocomposites.

Acknowledgments This research was supported by WCU (World Class University) program (R32-2008-000-20003-0) through the National Research Foundation of Korea funded by the Ministry of Education, Science and Technology.

References

1. E.P. Giannelis, R. Krishnamoorti, E. Manias, Adv. Polym. Sci. **138**, 107–147 (1999)
2. C. Zeng, L.J. Lee, Macromolecules **34**, 4098–4103 (2001)
3. J. Zhu, F.M. Uhl, A.B. Morgan, C.A. Wilkie, Chem. Mater. **12**, 4649–4654 (2001)
4. T. Sun, J.M. Garces, Adv. Mater. **14**, 128–130 (2002)
5. J.G. Dor, I. Cho, Polym. Bull. **41**, 511–518 (1998)
6. H.A. Essawy, A.S. Badran, A.M. Youssef, A.E.-.F.A.A. El-Hakim, Macromol. Chem. Phys. **205**, 2366–2370 (2004)
7. H. Chen, K. Yao, J. Tai, J. Appl. Polym. Sci. **73**, 425–430 (1999)
8. H.A. Essawy, Colloid Polym. Sci. **286**, 795–803 (2008)
9. T. Agag, T. Koga, T. Takeichi, Polymer **42**, 3399–3408 (2001)
10. N. Salahaddin, A. Moet, A. Hiltner, E. Baer, Eur. Polym. Mater. **38**, 1477–1482 (2002)
11. B. Dietrich, J. Vinyl Addit. Technol. **4**, 168–176 (2001)
12. L. Chazeau, J.Y. Cavaille, J. Perez, J. Polym. Sci., Part B: Polym. Phys. **38**, 383 (2000)
13. H. Imanishi, T. Yamaguchi, N. Fukuda, Jpn. J. Polym. Sci. Technol. **57**, 590–595 (2000)
14. D.Y. Wang, D. Parlow, Q. Yao, C.A. Wilkie, J. Vinyl Addit. Technol. **7**, 203–213 (2001)
15. M.E. Landis, A.B. Aufdembrink, P. Chu, I.D. Johnson, G.W. Kirker, M.K. Rubin, J. Am. Chem. Soc. **113**, 3189–3190 (1991)
16. O.Y. Kwon, K.W. Park, J. Ind. Eng. Chem. **7**, 44–49 (2001)
17. A. Galarneau, A. Barodawalla, T.J. Pinnavaia, Nature **374**, 529–531 (1995)
18. A. Bhaumik, T. Tatsumi, J. Catal. **182**, 349–356 (1999)
19. M. Sasidharan, A. Bhaumik, J. Mol. Catal. A: Chem. **328**, 60–67 (2010)
20. K.W. Park, Micropor. Mesopor. Mater. **127**, 142–146 (2010)
21. M.A. Roberts, G. Sankar, J.M. Thomas, R.H. Jones, H. Du, M. Fang, J. Chen, W. Pang, R. Xu, Nature **381**, 401–404 (1996)
22. S. Ferdov, V. Kostov-kytin, O. Petrov, Chem. Commun. **178**, 6–1787 (2002)
23. R. Murugavel, H.W. Roesky, Angew. Chem. Int. Ed. Engl. **36**, 477–479 (1997)
24. K.W. Park, J.H. Jung, J.D. Kim, S.K. Kim, O.Y. Kwon, Micropor. Mesopor. Mater. **118**, 100–105 (2009)